JOURNAL OF CATALYSIS 151, 111–124 (1995)

CO_2 Methanation under Transient and Steady-State Conditions over Rh/CeO_2 and CeO_2-Promoted Rh/SiO_2: The Role of Surface and Bulk Ceria

Alessandro Trovarelli,*,[1] Carla de Leitenburg,* Giuliano Dolcetti,* and Jordi LLorca†

*Dipartimento di Scienze e Tecnologie Chimiche, Università di Udine, via Cotonificio 108, 33100 Udine, Italy; and †Departament de Química Inorgànica, Universitat de Barcelona, Diagonal 647, 08028-Barcelona, Spain

Received February 24, 1994; revised June 3, 1994

A series of Rh/SiO_2 samples promoted with CeO_2 have been prepared and used as catalyst in CO_2 methanation. Their behaviour has been compared to that of unpromoted Rh/SiO_2 and Rh/CeO_2 catalysts. The activity has been monitored under transient and steady-state conditions and the catalysts have been characterized using quantitative temperature programmed reduction, chemisorption, X-ray diffraction, and transmission electron microscopy. By impregnation of amorphous silica with $Ce(NO_3)_3 \cdot 6H_2O$ followed by calcination at 923 K, aggregates of CeO_2 particles with size ranging from 35 to 150 nm (depending on initial cerium loading) form on the surface. These large agglomerates are constituted by individual, smaller (5–15 nm), crystalline CeO_2 particles. Redispersion of CeO_2 in the presence of H_2 at 773 K is observed in all samples. The presence of Rh, deposited by impregnation from $RhCl_3 \cdot 3H_2O$ solutions, accelerates the process. The reducibility of ceria is strongly enhanced by deposition on silica: complete reduction to Ce_2O_3 is observed for CeO_2-supported samples at temperatures lower than 1100 K, while a maximum of 50% reduction (corresponding to $CeO_{1.75}$) is observed for unsupported CeO_2 in the range of temperature 295–1400 K. The activity of the virgin catalyst, as tested under unsteady-state conditions, is positively influenced by the reduction temperature and CeO_2 crystallite size. We suggest that the observed enhancement of catalytic activity is linked to the presence of bulk vacancies created on ceria after reduction at high temperatures. Annihilation of these oxygen vacancies by oxygen from CO_2, under reaction conditions, restores the normal catalytic behaviour.

INTRODUCTION

Cerium-based catalysts in the presence of transition metals have been increasingly investigated in recent years because of their potential interest in several processes, from application in the treatment of exhaust gas from automobiles (1–3) to their use in methanation and methanol formation (4, 5), the water gas shift reaction (6), and acetone hydrogenation (7). There are several reasons why CeO_2 has been successfully used as catalyst promoter or support, although it is very difficult to distinguish its role in most of the processes. CeO_2 has been found to improve the thermal stability of alumina (8), to promote the reduction of supported metals and stabilize their reduced state (1, 9), to change the properties of Group 8 and 9 metals through electronic interaction at the metal/oxide interface (10), and, especially in exhaust catalysts, the oxide can act as an oxygen storage component (2).

We have recently investigated the behaviour of Rh supported over different reducible oxides in the hydrogenation of CO_2 (11, 12). Among the oxides tested, CeO_2 appeared to be the most interesting owing to its specific behaviour (12). It was reported that, following a high temperature reduction, the catalytic activity of Rh/CeO_2 catalyst in CO and CO_2 hydrogenation is increased by several times, in contrast to the strong suppression of activity observed on Rh supported over other reducible oxides like TiO_2, Ta_2O_5, and Nb_2O_5 (12, 13). The same behaviour has also been observed with other CeO_2-supported noble metals (14), demonstrating the crucial role of the support in promoting the catalytic activation of CO and CO_2. The presence of oxygen vacancies created after a high temperature reduction was suggested to be responsible for the activation of CO moieties at the interface between CeO_2 and Rh crystallites. However, some unsolved issues were still present in those studies; for example, the amount of surface and bulk vacancies formed after different reduction treatments and their role in the observed catalytic properties were not clearly understood. To further investigate the role of CeO_2 in these reactions, and particularly to address the above-mentioned points, we report here the effect of adding CeO_2 as a catalyst modifier to a high surface area Rh/SiO_2 catalyst. The catalytic activity in CO_2 methanation has been monitored under transient and steady-state conditions

[1] E-mail: trovarelli@dstc.uniud.it.

0021-9517/95 $6.00

and the catalysts have been characterized by H_2 chemisorption, temperature programmed reduction (TPR), X-ray diffraction (XRD), transmission electron microscopy (TEM), electron microdiffraction (ED), and energy dispersive X-ray analysis (EDX).

EXPERIMENTAL

Materials

CeO_2 was prepared by adding dropwise NH_4OH 0.1 *M* to a solution of $Ce(NO_3)_3 \cdot 6H_2O$. The resulting oxide was filtered, dried at 373 K for 15 h, calcined at 773 K, and then stored. SiO_2 was purchased from Merck. CeO_2/SiO_2 samples with different CeO_2 contents were prepared by wetting the silica support with a solution of $Ce(NO_3)_3 \cdot 6H_2O$ until incipient wetness followed by drying at 373 K for 15 h and calcination at 923 K for 2 h. The properties of all these samples are listed in Table 1. Rh samples were prepared by wetting the support with $RhCl_3 \cdot 3H_2O$ solution until incipient wetness, followed by drying at 373 K for 15 h and calcination at 773 K for 2 h. The gases used in the catalytic reactions (CO_2, H_2, He, $CO_2/H_2/He$, Ar/H_2) were of commercial purity, research grade. H_2 and He were further purified by passing through molecular sieves and oxygen traps (Alltech).

Catalytic Experiments

Catalytic experiments in continuous conditions were carried out in a stainless steel flow microreactor (length 13 cm, i.d. 6 mm) interfaced to a Hewlett–Packard HP5890A gas chromatograph equipped with thermal conductivity and flame ionization detectors. The amount of catalyst used was in the range 0.1–0.3 g. The ratio H_2/CO_2 in the reaction mixture was always 3/1 and no diluent was used. The system was operated at a total pressure of 1 atm. Space velocities were in the range 2500–5000 h^{-1} and CO_2 conversion was always less than 10%. A series of additional experiments in continuous conditions were made by using a CO_2(2%)/H_2(5.95%)/He(92.05%) mixture at very low CO_2/H_2 concentration.

TABLE 1

Characteristics of Ce/Si Samples

Sample	Ce (%)	CeO_2 (%)	μmol CeO_2/m^2	BET surface area (m^2/g)
A	0	0	—	580
B	1.3	1.6	0.15	610
C	4.7	5.8	0.57	585
D	12.7	15.6	1.70	532
E	23.1	28.4	4.02	410
F	81.4	100	—	18

In this configuration a U-shaped quartz reactor (6 mm i.d., 200 mm long) was used. The reactor was heated by an external oven and the temperature was monitored by using a thermocouple immersed in the catalyst bed. The amount of catalyst used was in the range 80–150 mg and the space velocities were 7,500–10,000 h^{-1}. Methane evolved was directly and continually monitored by using a flame ionization detector; the time delay between introduction of the reactants and monitoring of the products was less than 15 s. The system was calibrated by using CH_4/He mixtures with known CH_4 concentration.

Pulse experiments were carried out by using a micropulse reactor (i.d. 2.6 mm, 100 mm long). A pulse of CO_2 (10–100 μl) was injected upstream of the reactor in flowing H_2 by means of a six-way valve. The pulse passed through the microreactor and entered directly into the gas chromatograph. CH_4, CO_2, and water were separated in a Porapak Q column and then analyzed with TCD for conversion measurements; CH_4 was also directly analyzed with a flame ionization detector for peak shape analysis. The amount of catalyst used was in the range 5–15 mg. Turnover numbers were calculated by using the method described by Mori *et al.* (15). In all cases the catalytic activity was investigated following the reduction in hydrogen at 473 K for 2 h (low temperature reduction, LTR), and at 773 K for 2 h (high temperature reduction, HTR).

Catalyst Characterization

BET surface areas and H_2 uptake were measured with a Carlo Erba Sorptomatic 1900 instrument; H_2 chemisorption at 298 K was calculated by extrapolating at zero pressure the linear part of the isotherm. Temperature programmed reduction was performed in a conventional, U-shaped, quartz microreactor (i.d. = 6 mm, l = 200 mm) using a 5% H_2 in argon mixture flowing at 35 cm^3/min (STP). For TPR measurements the temperature range investigated was 295–1400 K and the heating rate was always 10 K/min. The reduction of CuO to metallic copper has been used to calibrate the TPR apparatus for H_2 consumption.

X-ray diffraction patterns of powders were collected with an Inel instrument using Co radiation. The average CeO_2 crystal size has been determined by using the Scherrer formula $L = \lambda K/(\beta \cos \theta)$, where λ is the X-ray wavelength (λ = 1.78897 Å), K is a constant (0.9), θ is the angle of reflection, and β represents the measured peak width (FWHM). All CeO_2 reflections (excluding low intensity signals) have been used and averaged for a more accurate calculation of mean crystal size. Samples for TEM and ED were suspended to form a slightly turbid suspension in methanol. Each suspension was constantly agitated in an ultrasonic bath. A drop of the suspension

was placed on a carbon-coated copper grid. The alcohol evaporated, leaving a film of catalyst particles on the grid, which was then loaded into a Hitachi H 800-MT transmission electron microscope. The operating voltage was 150 kV. Energy dispersive X-ray analysis was carried out in STEM mode with a Kevex 8000 quantum system. The X-rays emitted from the specimen upon electron irradiation were collected in the range 0–40 KeV for 100 s.

RESULTS

Temperature Programmed Reduction

TPR profiles of unsupported CeO_2 and a series of CeO_2/SiO_2 samples of increasing CeO_2 concentration are shown in Fig. 1. For pure CeO_2 (Fig. 1a) two peaks are detected at approximately 810 and 1100 K and a shoulder at around 760 K. The main features of TPR traces are maintained also with CeO_2/SiO_2 sample (Fig. 1b–1e) in which at least two different components are observed, one peaking around 800 K and the other in the range 1020–1050 K. By decreasing CeO_2 loading a shift toward lower temperatures is observed for the high temperature signal (Table 2), while for the first peak smaller deviations from the temperature of 800 K (from 818 to 794 K) are observed, which are not depending on CeO_2 loading. Moreover, for CeO_2 loading lower than 5.8 wt.% an inversion of the intensity of the two peaks is observed. A quantitative analysis of TPR profiles has been undertaken in order to determine the extent of reduction and to give a better assignment of each reduction step. Reduction of CuO to metallic Cu (16) has been used to calibrate the TPR apparatus for H_2 consumption. Reaction [1] was used to calculate the theoretical amount of hydrogen consumed for reduction of CeO_2 to Ce_2O_3 in CeO_2, CeO_2/SiO_2, and $Rh/CeO_2/SiO_2$ samples, and Eq. [2] (17) was used to calculate the amount of hydrogen consumed for Rh_2O_3 reduction to Rh in $Rh/CeO_2/SiO_2$ samples:

$$2CeO_2 + H_2 = Ce_2O_3 + H_2O \quad [1]$$

$$Rh_2O_3 + 3H_2 = 2Rh + 3H_2O. \quad [2]$$

The difference between experimental and calculated values (Table 2) is always lower than 8% and the reproducibility of TPR analysis for different batches of the same sample is within 7%. These quantitative results also provide indirect evidence that other side effects, which could affect TPR of high surface area CeO_2 (18), are absent here.

It is shown that for silica-supported samples, reduction of CeO_2 to Ce_2O_3 is complete at temperatures lower than 1100 K, whereas higher temperatures are required to reduce pure ceria. In the temperature range investigated (300–1400 K) a maximum reduction of 50% can be

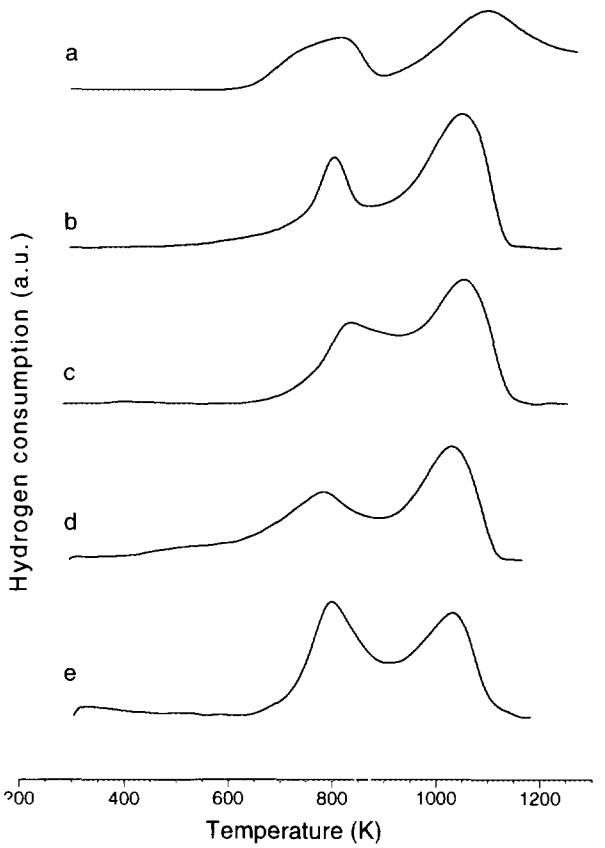

FIG. 1. Temperature programmed reduction of (a) CeO_2, (b) $CeO_2(28.4\%)/SiO_2$, (c) $CeO_2(15.6\%)/SiO_2$, (d) $CeO_2(5.8\%)/SiO_2$, and (e) $CeO_2(1.6\%)/SiO_2$. For clarity the area of the curves has been normalized.

TABLE 2

Hydrogen Consumed and Peak Positions in Temperature Programmed Reduction

Sample	H_2 consumed[a]		Peak temperature (K)
	Calculated	Experimental	
CeO_2	1162	558	808, 1098
$CeO_2(28.4\%)/SiO_2$	330	325	803, 1051
$CeO_2(15.6\%)/SiO_2$	181	190	818, 1050
$CeO_2(5.8\%)/SiO_2$	67	63	794, 1028
$CeO_2(1.6\%)/SiO_2$	19	20	798, 1031
Rh/CeO_2	1220	697	400, 699, 1095
$Rh/CeO_2(28.4\%)/SiO_2$	388	365	395, 589, 997
$Rh/CeO_2(15.6\%)/SiO_2$	239	249	415, 966
$Rh/CeO_2(5.8\%)/SiO_2$	125	135	401, 964
$Rh/CeO_2(1.6\%)/SiO_2$	77	65	385
Rh/SiO_2	58	61	398

[a] H_2 consumed (μmol) for reduction of 400 mg of catalyst.

reached with pure ceria, corresponding to an overall stoichiometry of $CeO_{1.75}$, a composition which is consistent with that calculated from the phase diagram for reduction of nonstoichiometric CeO_{2-x} at these temperatures (19). A correlation between the temperature and the extent of reduction for different samples is reported in Fig. 2. The reducibility of CeO_2 crystallites clearly increases by deposition on SiO_2 (Ce_2O_3 is completely formed at temperature of about 1100 K), and it is shown to be dependent on ceria loading (compare Fig. 2b and Fig. 2c).

The presence of Rh modifies the features of TPR profiles (Fig. 3a–3f). A sharp signal centered around 350–400 K is observed in all samples. In agreement with several authors (2, 8, 20), these maxima can be associated with the reduction of rhodium oxides and probably with the reduction of the most readily reducible surface oxygen on the ceria support, adjacent to the metal. It is well known that Rh can activate H_2 which subsequently can spill over to the support, promoting support reduction at lower temperatures (20, 21). Direct evidence that this phenomenon occurs under our conditions, even on mixed oxide samples, is the fact that on increasing CeO_2 content, an increase in the amount of H_2 consumed at low temperatures is observed. The value of total hydrogen consumption for Rh reduction as calculated by integrating the peaks centered around 400 K is well above the stoichiometric value calculated for Rh on undoped silica. If we set to 1 the value of H_2 consumed for Rh reduction in Rh/SiO_2, calculated by integrating the area of the corresponding peak (Fig. 3f), it becomes 1.4 for $Rh/CeO_2(1.6\%)/SiO_2$, 2 for samples containing 5.8 wt.% of CeO_2, 2.8 and 3 for samples containing respectively 15.6 and 28.4 wt.% of ceria; this indicates that the more CeO_2 becomes available to the surface the more H_2 is being split over and consumed for the reduction. Notably with the more disperse samples, most of the H_2 consumption for CeO_2 reduction is concentrated at temperatures lower than 500 K. The effect of Rh on CeO_2 reduction is well illustrated in Figs. 2d–2f. These curves have been obtained by subtracting from the TPR of the corresponding samples the amount of H_2 consumed for Rh reduction in Rh/SiO_2 and then integrating the curves. There is evidence that reduction of the support at low temperatures is dramatically influenced by the presence of Rh and by CeO_2 loading. With the more disperse samples almost 70% of CeO_2 reduction is observed at temperatures lower than 500 K.

The profile of the medium and high temperature region also differs from that obtained without the metal. Gener-

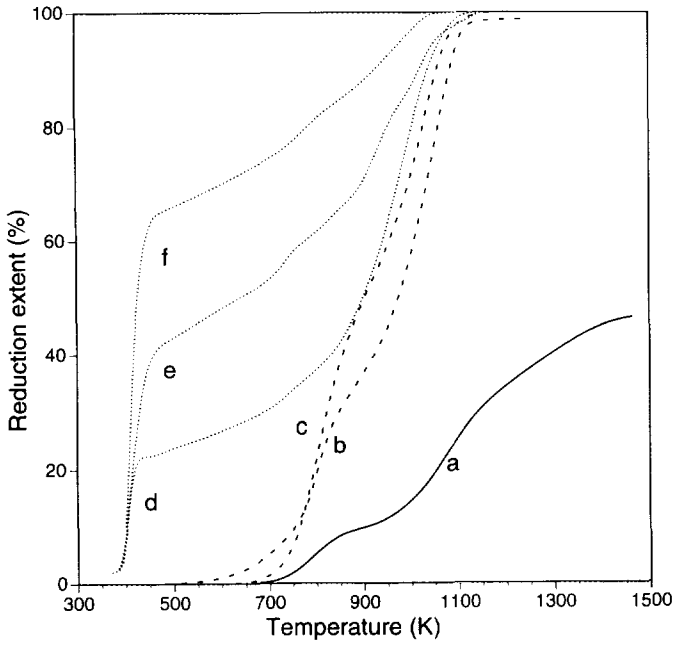

FIG. 2. Extent of CeO_2 reduction vs temperature for (a) CeO_2, (b) $CeO_2(28.4\%)/SiO_2$, (c) $CeO_2(1.6\%)/SiO_2$, (d) $Rh/CeO_2(28.4\%)/SiO_2$, (e) $Rh/CeO_2(5.8\%)/SiO_2$, and (f) $Rh/CeO_2(1.6\%)/SiO_2$.

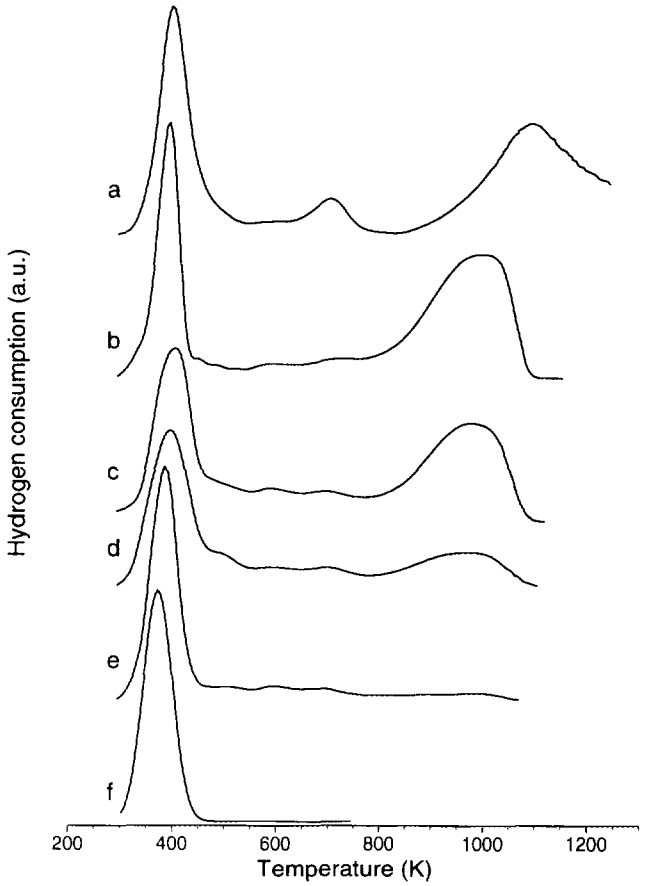

FIG. 3. Temperature programmed reduction of (a) Rh/CeO_2, (b) $Rh/CeO_2(28.4\%)/SiO_2$, (c) $Rh/CeO_2(15.6\%)/SiO_2$, (d) $Rh/CeO_2(5.8\%)/SiO_2$, (e) $Rh/CeO_2(1.6\%)/SiO_2$, and (f) Rh/SiO_2. For clarity the area of the curves has been normalized.

ally, as can be seen from Fig. 3, a visible shift in the direction of lower temperatures is observed with a general broadening of the signal which makes it very difficult to separate each contribution. Only for samples with CeO_2 concentration 5.8% or higher are there still appreciable contributions at high temperature.

An additional experiment has been carried out on the $Rh/CeO_2(28.4\%)/SiO_2$ sample, in order to estimate the degree of CeO_2 reduction after prolonged H_2 treatment. The reduction conditions were similar to those used for prereduction in the catalytic experiments described below. The sample has been reduced at 473 and 773 K for 2 h; after each reduction a TPR has been performed on the reduced sample and the results are reported in Fig. 4. A quantitative estimate of H_2 consumption led to a composition of CeO_x with $x = 1.8$ after LTR and 1.77 after HTR.

Electron Microscopy

All samples have also been characterized with X-ray diffraction, transmission electron microscopy, electron microdiffraction, and energy dispersive X-ray analysis. It is observed that by impregnation of $Ce(NO_3)_3$ on SiO_2 and subsequent heating at 923 K, large CeO_2 agglomerates, ranging in size from 36 to 152 nm, depending on CeO_2 loading, are formed on the surface (see Table 3). In Fig. 5a is reported a micrograph of $CeO_2(5.8\%)/SiO_2$ showing the large, round CeO_2 patches. However, a careful examination of these aggregates shows that they are constituted of smaller, individual crystalline CeO_2 particles with size ranging from 5 to 15 nm. Notably, the size

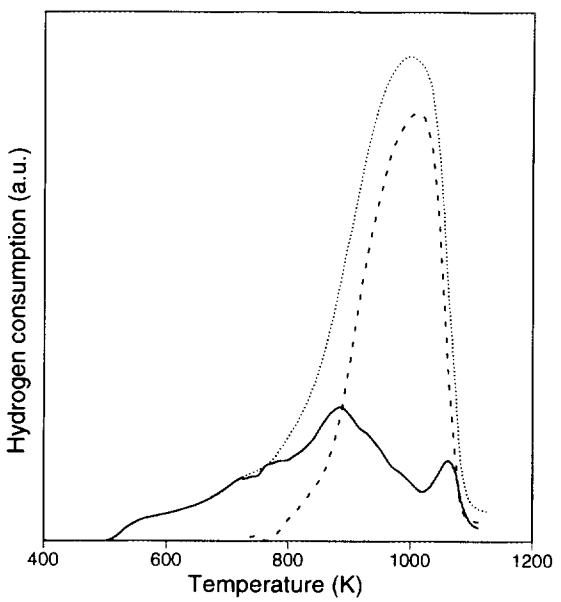

FIG. 4. Temperature programmed reduction of $Rh/CeO_2(28.4\%)/SiO_2$ after reduction for 2 h at 473 K (· · ·) and 773 K (- - -). The solid line represents the difference between the two curves.

TABLE 3

CeO_2 Particle Size Dimensions (nm) as Calculated by TEM and XRD Analysis

Samples	Not treated[a] TEM	Not treated[a] XRD	Treated in H_2 at 773 K TEM	Samples with 1% Rh reduced in H_2 at 773 K TEM
$CeO_2(28.4\%)/SiO_2$	15(152)[b]	12	15(142)	13
$CeO_2(15.6\%)/SiO_2$	13(140)	11	13(122)	10
$CeO_2(5.8\%)/SiO_2$	13(99)	10	13(78)	8
$CeO_2(1.6\%)/SiO_2$	5(36)	ND	[c]	2
CeO_2	24	22	—	25

Note. ND, not detected.

[a] The values refer to CeO_2/SiO_2 samples after calcination at 923 K (see text for sample preparation).

[b] Average crystal size. Mean agglomerate size is given in parentheses.

[c] Filamentary appearance.

of these crystallites is not strongly affected by the amount of CeO_2 present at high CeO_2 loading (>1.7 wt.%). X-ray diffraction analysis confirms the presence of small CeO_2 particles and the accordance between TEM and XRD is within 20% (Table 3). The effect of H_2 treatment at 773 K is shown to affect the main particle size but not the dimensions of individual crystallites. It appears from the data reported in Table 3 that the large CeO_2 agglomerates formed at CeO_2 loading >1.7% redisperse on the support when heated in H_2. A micrograph showing how large agglomerates redisperse in H_2 is reported in Fig. 5b for the $CeO_2(5.8\%)/SiO_2$ sample treated in H_2 at 773 K. The micrograph also shows in more detail how individual crystallites agglomerate into larger particles; in this case, individual CeO_2 crystallites with approximate size of 13 nm agglomerate into particles with mean size of 78 nm. On the other hand, CeO_2 electron diffraction lines fade after H_2 treatment at 773 K, especially in low CeO_2 content samples, indicating that at this temperature partial reduction of CeO_2 into an amorphous phase occurs. The redispersion phenomenon is drastically exhibited by the low CeO_2 content sample $CeO_2(1.6\%)/SiO_2$, as shown by the micrograph in Fig. 5c. In this micrograph, a filamentous structure of CeO_2 well spread over SiO_2 is visible, which indicates a stronger interaction between CeO_2 and the support after H_2 treatment.

The presence of Rh affects the sample morphology. While the results for $Rh/CeO_2/SiO_2$ before reduction were indistinguishable from those reported for CeO_2/SiO_2 (except for the presence of Rh_2O_3), $Rh/CeO_2/SiO_2$ samples after reduction in hydrogen at 773 K do not show the presence of large CeO_2 agglomerates. Only a few agglomerates have been detected and CeO_2 is present mainly as

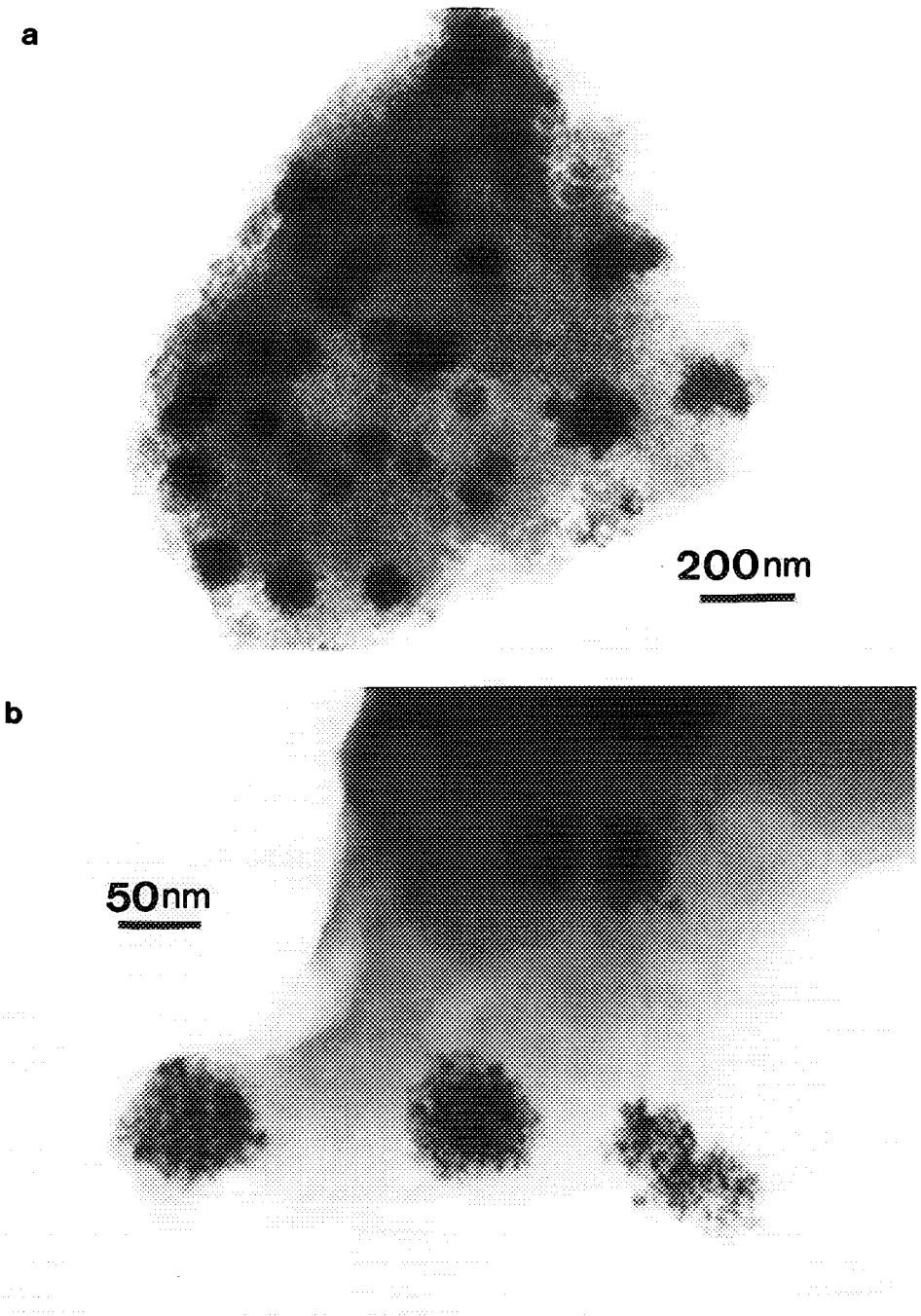

FIG. 5. Electron micrographs of CeO_2(5.8%)/SiO_2 sample before (a) and after (b) hydrogen treatment at 773 K, (c) CeO_2(1.6%)/SiO_2 sample treated in hydrogen at 773 K, and (d) Rh/CeO_2(5.8%)/SiO_2 sample after hydrogen treatment at 773 K.

individual crystallites on the surface. This is illustrated in Fig. 5d, which shows a micrograph of the Rh/CeO_2(5.8%)/SiO_2 sample treated in hydrogen at 773 K. EDX traces obtained from different areas of each Rh-containing catalyst indicate that Rh is preferentially located on CeO_2-rich areas, but not on SiO_2. Samples containing Rh exhibit smaller CeO_2 crystal size with respect to the homologous samples without Rh, as summarized in Table 3; in addition, and at variance with previous samples, the dimension of the crystallites depends on CeO_2 loading. A redispersion effect in the presence of H_2 has already been observed in similar systems (22–24). For example, at 770 K, CeO_2 particles redisperse and spread over SiO_2 in powder CeO_2/SiO_2 and Pt–CeO_2/SiO_2 sam-

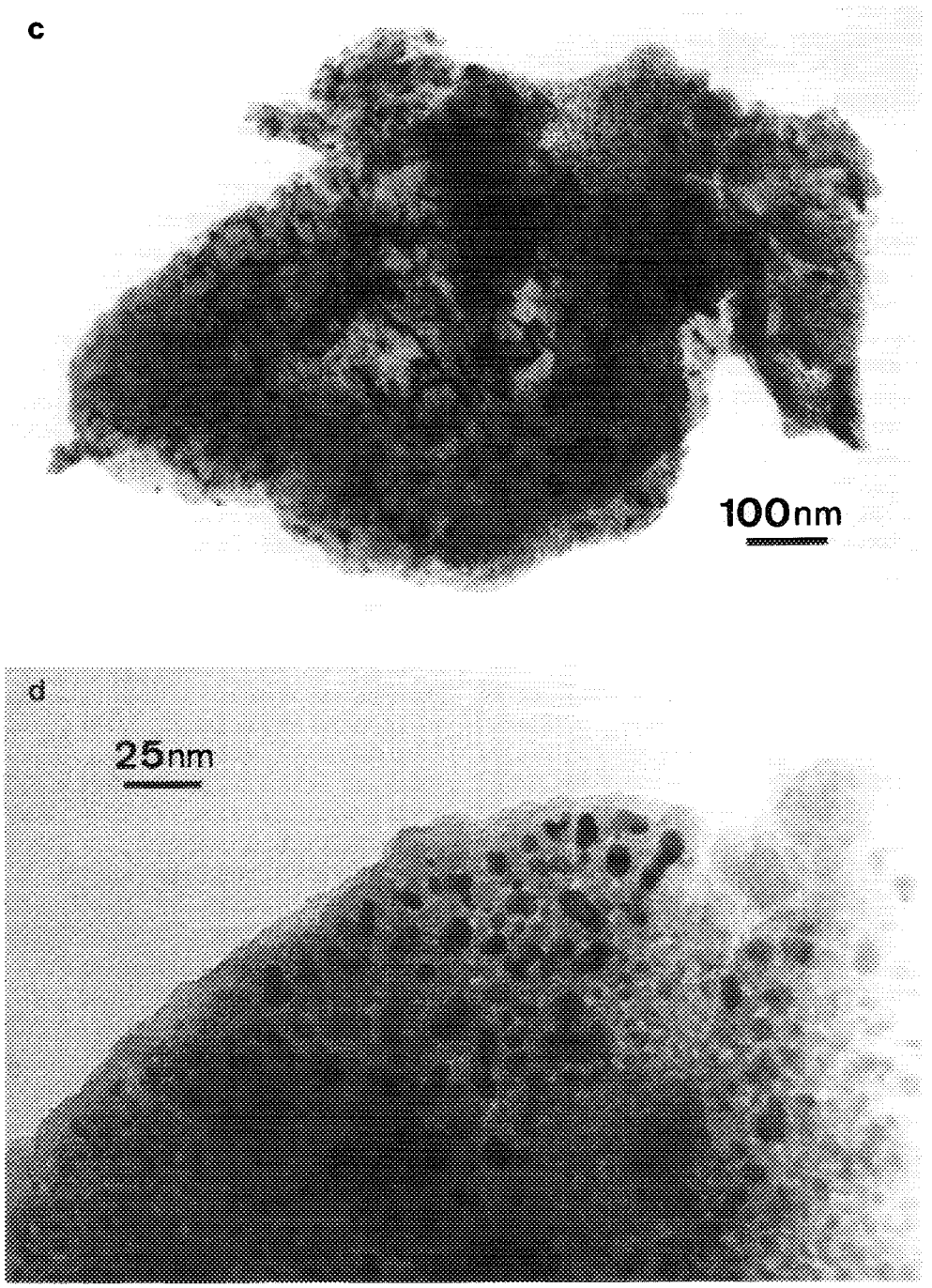

FIG. 5—*Continued*

ples (22); a partial amorphization has also been observed. The same effect has also been reported by Krause *et al.* (24), which showed that in a model, thin film Rh–Ce/SiO_2 system, small CeO_2 particles in contact with SiO_2 redisperse in H_2 at 870 K. They also reported formation of cerium silicates after H_2 treatment of CeO_2/SiO_2 at 1073 K; moreover, the presence of Rh was shown to lower the temperature of formation of $Ce_2Si_2O_7$ to 870 K. In our case, for all samples, no evidence for $Ce_2Si_2O_7$ was detected in the electron diffraction patterns after treatment in H_2 at 773 K. Similarly, with $Pt/CeO_2/SiO_2$ samples no evidence was found for silicate formation at these temperatures (22). The reason for the difference is most probably due to the higher temperatures used by Krause

et al., though other factors such as sample treatment and preparation could affect this result as well.

In the case of pure CeO_2, crystallite size is not affected by treatment under H_2 at 773 K and/or by the presence of Rh.

CO_2 Methanation

The effect of addition of cerium oxide for samples containing 1% Rh on silica in the methanation of carbon dioxide has been studied. All samples were tested at atmospheric pressure under transient and continuous conditions following a low (473 K, 2 h) and a high (773 K, 2 h) temperature reduction. Our main concern was to study the effect of reduction temperature on CO_2 methanation activity and particularly to gain some evidence on the role played by CeO_2. We have used three different approaches: (1) catalytic tests under steady-state continuous conditions; (2) activity under transient conditions by using a pulse reactor; (3) catalytic activity under continuous conditions but using a very dilute CO_2/H_2 mixture. Unless otherwise stated, all the activities are in (μmol) $[(g_{cat})\ (h)]^{-1}$. We avoided, when possible, the use of turnover numbers, which can be easily calculated from the Rh dispersions given in Table 4. It is very well known that CO and especially H_2 chemisorption cannot be used to correctly estimate Rh dispersion in ceria-containing samples (7, 9, 13, 25). The occurrence of H_2 spillover leads to an overestimate of hydrogen uptake; this can also be seen from our chemisorption measurements, in which the higher is the CeO_2 loading, the higher is the H_2 uptake. CO uptake by Rh/CeO_2 can also lead to inaccurate evaluation of Rh dispersions owing to significant CO adsorption by the support (13) and strong dependence of CO adsorption on reduction temperature (13, 20).

The results obtained under continuous conditions are briefly summarized in Fig. 6. By deposition of CeO_2, an increase in the rate of methane formation is observed after both LTR and HTR, which reaches a maximum for samples containing 1.6 wt.% of CeO_2. By increasing CeO_2 loading, the overall activity decreases. For LTR samples the activity stabilizes at values slightly higher than those observed for Rh/SiO_2, while for HTR samples the difference in activity is less marked and the rate of methane formation in Rh/SiO_2 is slightly higher than for the $Rh/CeO_2(28.4\%)/SiO_2$ sample. The steady-state activity is lower after a high temperature reduction in all samples and the promotional effect following CeO_2 addition is more moderate. The behaviour observed for CO_2 methanation under transient conditions over $Rh/CeO_2/SiO_2$ samples is reported in Table 4. After reduction at 473 K for 2 h, methanation activity is constant with pulse number and water is normally detected at the outlet as a reaction product. In accordance with steady-state measurements, deposition of CeO_2 results in a higher catalytic activity, reaching a maximum for the $Rh/CeO_2(1.6\%)/SiO_2$ sample. Following HTR, for samples with ceria content higher than 5.8 wt.%, an enhancement of reaction rate is observed; however, this enhancement is not constant and in the following pulses the catalytic activity decreases, stabilizing after several pulses at values which are similar to those observed after LTR. Notably, water is not detected as a reaction product in the samples in which an enhancement is observed. It is detected only after few pulses, in parallel with the decrease of activity.

The catalytic activity has also been monitored by using a $H_2/CO_2/He$ mixture at very low CO_2/H_2 concentration, in order to minimize the effect of reactants and products on catalyst modification. We expected to find a condition under which the catalytic activity enhancement observed

TABLE 4

CO_2 Methanation over Rh/CeO_2 and $Rh/CeO_2/SiO_2$ Samples in Pulse Conditions[a]

	Low temp. reduction		High temp. reduction				
			TN				
Sample[b]	TN[c]	H/Rh[d]	Pulse 1	Pulse 2	Pulse 3	After n pulses[e]	H/Rh
A	36	33	35	32	36	31	55
B	200	46	70	68	67	66	62
C	140	51	50	50	51	51	71
D	51	62	83	69	66	49	67
E	54	71	257	159	82	40	60
F	130	90	3200	2860	2550	39	57

[a] Reaction conditions: Temperature 463 K, pulse size: 20 μl.
[b] For sample designation see Table 1.
[c] TN: mol CH_4 (mol Rh)$^{-1}$ s^{-1} $\times$ 10^4.
[d] H/Rh values as calculated by measuring H_2 chemisorption.
[e] n depends on samples (from n = 5 for sample A to n = 14 for sample F).

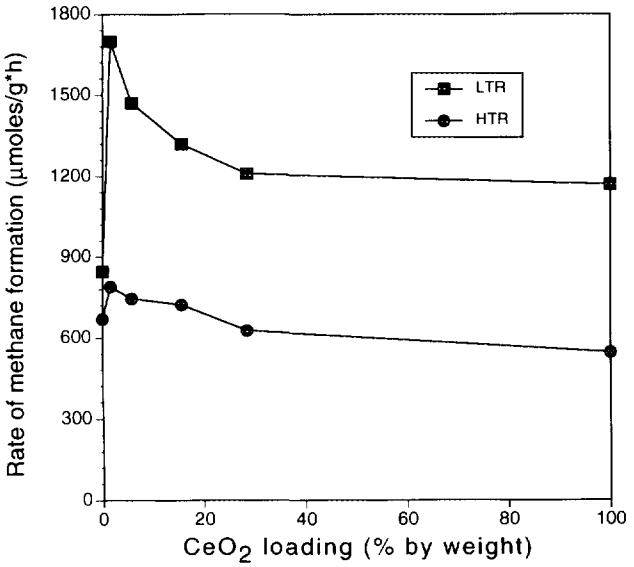

FIG. 6. CO_2 methanation in continuous conditions at 500 K: Methane formation rate vs CeO_2/SiO_2 loading; (■) reduction temperature 500 K (LTR), (●) reduction temperature 773 K (HTR).

in pulse conditions could also be detected in continuous conditions, thus allowing a more simple and direct interpretation and manipulation of data. The continuous and rapid monitoring of CH_4 evolved, plus the use of very dilute mixture, allowed us to detect transient evolution of the catalyst which cannot be detected by using a conventional continuous system (characterized by higher concentration of reactants and products, and periodical GC analysis of effluents). The results obtained are very interesting and are summarized in Table 5. In Fig. 7 is also

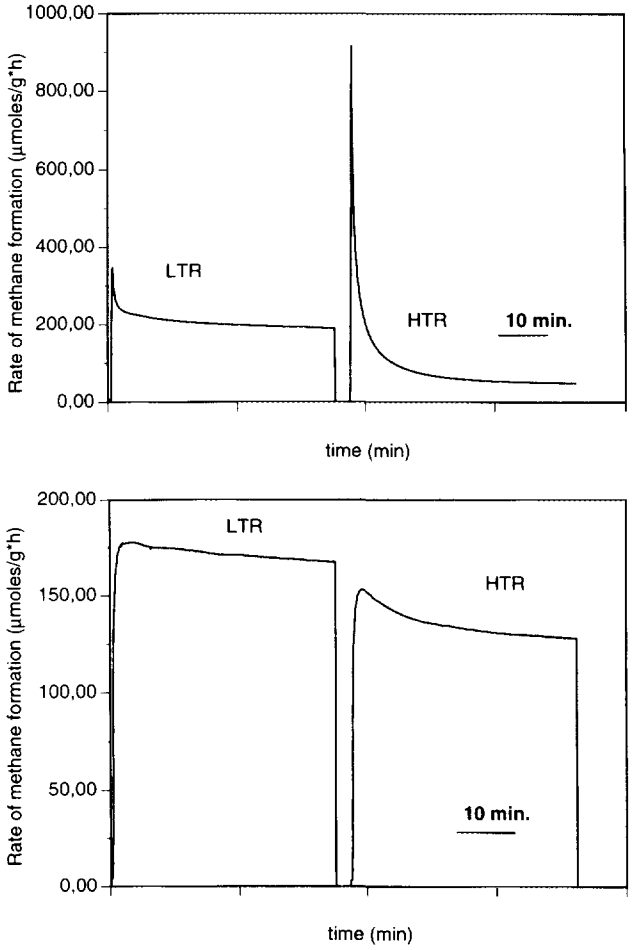

FIG. 7. Rate of CH_4 formation vs time for $Rh/CeO_2(28.4\%)/SiO_2$ (upper) and $RhCeO_2(5.8\%)/SiO_2$ (lower) samples following LTR and HTR. (See text for details on how the experiments have been conducted.)

TABLE 5

Methanation of CO_2 Using a Preformed ($CO_2/H_2/He$ = 2/5.95/92.05) Mixture and Analyzing Directly Methane Evolved[a]

Sample	Low temp. reduction (473 K)			High temp. reduction (773 K)		
	Time[b]	Rate[c]	Deact. (%)[d]	Time[b]	Rate[c]	Deact. (%)[d]
Rh/CeO_2	0.8	544	49.1	0.8	7788	99.6
$Rh/CeO_2(28.4\%)/SiO_2$	0.6	348	45.7	0.4	917	94.6
$Rh/CeO_2(15.6\%)/SiO_2$	0.9	189	29.1	0.6	211	57.3
$Rh/CeO_2(5.8\%)/SiO_2$	1.9	177	22.1	2.16	153	16.3
$Rh/CeO_2(1.6\%)/SiO_2$	2.3	309	17.4	2.5	238	9.3
Rh/SiO_2	6.5	80	4.4	3.7	89	8.7

[a] For details see Experimental.
[b] Time (min) at which the maximum activity is shown.
[c] Rate of CH_4 formation ($\mu mol/g_{cat.}$ h).
[d] Percent of deactivation after 35 min of reaction [100 − (rate after 35 min/maximum rate) × 100].

reported, as a comparison, the time course of methane formation following a low and a high temperature reduction on $Rh/CeO_2(28.4\%)/SiO_2$ and $Rh/CeO_2(5.8\%)/SiO_2$ samples. Time zero represents the time at which the CO_2/H_2 mixture is introduced into the reactor. After approx. 15 s the catalytic activity starts, reaching a maximum after a few minutes (or a few seconds, depending on the samples), and then evolves to reach steady-state conditions. After a low temperature reduction Rh/CeO_2 is shown to be more active than Rh/SiO_2 but with a higher deactivation. By addition of small quantities of CeO_2, promotion of CH_4 formation is observed, which is also in agreement with the behaviour observed under pulse and steady-state conditions. Following a high temperature reduction, there is an increase in the catalytic activity of Rh/CeO_2 and $Rh/CeO_2(>5.8\%)/SiO_2$ samples, followed by a very rapid deactivation, which brings the catalyst back to a situation similar to that observed after LTR (the final activity is, however, much lower after HTR than after LTR). Deactivations as high as 99.6 and 94.6% are observed with Rh/CeO_2 and $Rh/CeO_2(28.4\%)/SiO_2$ samples after 35 min of reaction. After this time a total of approx. 850 μmol of CO_2 per gram of catalyst have passed through the reactor.

Summarizing our catalytic results, we have seen by using different techniques that two different promotional effects are present in these systems in relation to reduction temperature and CeO_2 loading. The presence of CeO_2 in a disperse phase, as small crystallites on the silica surface (CeO_2 loading lower than 5.8 wt.%), produces an increase in the methanation activity relative to that of undoped Rh/SiO_2. This is observed in transient and continuous conditions regardless of the reduction temperature. A quite different situation arises when the behaviour of the catalyst is investigated under unsteady-state conditions. In this case the activity is measured on a time scale of seconds and some information on the activity of the catalyst at the beginning of the reaction can be obtained. As can be seen, there is an increase in the activity of the ceria-containing samples after HTR, but only for CeO_2 loading >5.8 wt.%. However, the high activity does not stabilize and after a few pulses (or a few minutes, depending on reaction conditions) the activity drops to values similar to or lower than that observed after a LTR. There are four points that are worth mentioning: (i) the activity enhancement increases with CeO_2 content, and thus crystallite size, being maximum for Rh on pure CeO_2; (ii) the stronger is the enhancement of catalytic activity, the higher is the percentage of deactivation observed in the first 35 min of reaction; (iii) the activity enhancement is clearly observed only for samples of CeO_2 loading higher than 5.8 wt.% (and crystallite size larger than 80 Å); (iv) the activity enhancement is not observed after a low temperature reduction.

DISCUSSION

Let us first discuss some aspects of the TPR of CeO_2 and Rh/CeO_2 which can be useful to the interpretation of the reduction profiles of the CeO_2/SiO_2 system. The presence of two signals in the TPR of pure CeO_2 has been associated with a stepwise reduction of the oxide (2, 8, 24–27); however, a definitive and unambiguous discrimination between the various processes is still missing. While the origin of the second peak, which has been attributed to reduction of the bulk of oxide crystallites, is clear, less clear and open to different interpretations is the origin of the first signal. Yao and Yao (2) attributed this peak to the reduction of the surface capping oxygen of CeO_2. They based their results on studies of the reduction of CeO_2 with different surface areas, and thus, different number of surface reducible sites. However, the range of surface area explored was only 1–10 m^2/g. Similar results were found later by Johnson and Mooi (26), who developed a model to calculate CeO_2 surface area from the H_2 consumed in the first peak. Again, this study was limited by the range of surface areas examined, which was 1–27 m^2/g. Besides, their results fit the model only for samples with surface area less than 13 m^2/g and other authors have reported an inconsistency in the application of this model to high surface area samples (18, 27). More recently other groups have assigned the first peak to different contributions from both reduction of easily reducible surface Ce^{IV} and formation of nonstoichiometric oxides CeO_{2-x} (28, 29). The indication that in our samples the relative intensities of the two peaks depend on CeO_2 loading in the way observed, along with a quantitative determination of the extent of reduction for each signal, is indicative of the fact that, *at least under the kinetic control of the TPR experiments*, formation of oxides with definite stoichiometries is not predominant. This, however, does not exclude the possibility of formation of nonstoichiometric oxides under isothermal conditions. Formation of $CeO_{1.84}$ has in fact been reported over Rh/CeO_2 after prolonged H_2 treatment at 623 K (28). The first TPR signal probably originates from reduction of small crystallites and/or reduction of the first surface layers of larger CeO_2 crystallites. It should be noted that while the peak temperature of the second signal varies by more than 50° from CeO_2 to CeO_2/SiO_2 samples (and 30° within supported samples), the peak temperature of the first signal is almost constant around 800 K, indicating that the maximum of H_2 consumption from the first peak is not greatly affected by the dimension of CeO_2 crystallites but is mainly due to surface Ce^{IV} reduction. Accordingly, a quantitative estimation of H_2 consumed in the first signals, as reported in Fig. 2, clearly indicates that the lower the CeO_2 loading, the higher is the percentage of CeO_2 reduction at lower temperatures.

It follows that the TPR traces in CeO_2/SiO_2 samples should reflect the reducibility of CeO_2 with different crystallite sizes and, as a consequence, a qualitative and quantitative analysis of TPR profiles can be used as a fingerprint to check the dispersion of CeO_2. For CeO_2 particle size larger than 10 nm, the TPR profiles are qualitatively similar to that observed for reduction of pure CeO_2. However, owing to the difference in CeO_2 particle size (10–15 nm for CeO_2/SiO_2 samples, 25 nm for CeO_2), the peak attributable to CeO_2–Ce_2O_3 reduction is observed at lower temperatures, and the reduction to Ce_2O_3 is complete. At low ceria loading, the small ceria crystallites formed (5 nm) are further dispersed on the silica surface under H_2 treatment, and, as a consequence, hydrogen consumption at high temperature for bulk CeO_2 reduction diminishes. This explains the inversion of the intensity of the two peaks for ceria loading lower than 5.8 wt.%. It is clearly shown in Fig. 2 that on increasing CeO_2 loading, and thus crystallite size, there is an increase in the resistance of the oxide to reduction, especially in the range 800–1100 K, where the reduction of bulk CeO_2 takes place. The presence of silica, which acts as a dispersing agent, also facilitates the complete reduction of CeO_2 deposited thereon, reducing sintering at very high temperatures which is probably the reason for the incomplete Ce(IV) reduction in pure CeO_2. We have indeed found that the surface area of CeO_2 after a TPR run is reduced by more than one order of magnitude, and much of this effect is concentrated above 1000 K. At high temperatures, other effects might also affect TPR traces; the reported formation of cerium silicates at temperatures higher than 1000 K (24) could be one of the reasons for the easier Ce(IV) reduction on SiO_2-supported samples.

The presence of Rh does modify the main features of TPR. For samples with low ceria loading (1.6 and 5.8 wt.%) H_2 consumption at high temperature is negligible, indicating that for these samples CeO_2 is redispersed over the support and reduction of bulk CeO_2 is negligible. This is in agreement with TEM and XRD measurements; in the presence of H_2, small CeO_2 crystallites with mean particle diameters of 20 and 80 Å are detected for 1.6 and 5.8 wt.% CeO_2 samples, respectively. Moreover, the effect of redispersion of CeO_2 in H_2 (particularly evident for the 1.6 wt.% sample) plus the strong H_2 spillover from Rh can explain the high degree of CeO_2 reduction at relatively low temperatures.

Catalytic Measurements

The role of the metal and the support in CO and CO_2 hydrogenation has been extensively studied in recent years; although the main effort has been focused on CO activation, there have also been different groups involved in the study of CO_2 hydrogenation (30). It has already been shown by the early fundamental work of Solymosi *et al.* (31) that the main product of CO_2 hydrogenation on supported Rh is methane, although some higher hydrocarbons can be formed in particular conditions over Rh supported on reducible supports (11).

The effect of addition of cerium on the catalytic properties of silica-supported noble metals has been studied by several authors (23, 32–34). These studies were also mainly focused on the catalytic properties in the activation of CO. It was generally observed that small quantities of Ce cause a marked improvement in the activity and selectivity of CO hydrogenation. For example, in Pd/SiO_2 catalyst, decoration of Pd by rare earth oxide moieties aids the dissociation of CO and raises the methanation activity relative to that of unsupported Pd/SiO_2 (33). The activity to CH_3OH is increased as well. The addition of Ce to a Rh/SiO_2 catalyst increases the rate of formation of higher molecular weight products and olefins in CO hydrogenation (23); this promotional effect is observed regardless of the pretreatment of the catalyst. Kienneman *et al.* reported an increase in the selectivity for ethanol when Ce is added to a Rh/SiO_2 catalyst (32).

The presence of Ce^{3+} on the surface and the electronic interaction with Rh have been proposed to account for such behaviour. A mechanism which is similar to that proposed with other reducible oxide-supported metals in which the active sites are present at the interface between the metal and the reduced support is believed to be responsible for the high activity in CO/hydrogen reactions (5, 35). A decoration of the metal particles by reduced CeO_2 followed by an electronic interaction has been proposed in the case of Pd (33). However, recent results (12, 13, 25) do not seem to support the fact that, at least with Rh, the system enters into a classical strong metal-support interaction (SMSI) state as it was originally defined (36), though a conclusive and unequivocal answer is still missing.

In all of the above-considered examples, the Ce loading is always below 5%, and there is no systematic study on the effect of Ce content on the catalytic activity.

We have recently reported, as a part of a systematic study on CO_2 hydrogenation on different reducible oxides, that the high temperature reduction at 773 K of Rh/CeO_2 catalysts induced a transient Rh–CeO_2 interaction which enhances the rate of CO and CO_2 hydrogenation (12). The presence of surface vacancies generated after high temperature reduction and their interaction with the CO moiety were suggested to be responsible for promoting the activation (13). The present observations, carried out on CeO_2-promoted Rh/silica, indicate that not all the samples are active in promoting the enhancement in CO_2 methanation after a HTR, but only samples with large ceria crystallites, which could be indicative of the partici-

pation, at some level, of bulk CeO_2 in the observed surface properties. We have seen that the relative amount of surface and bulk vacancies which can be formed on CeO_2 is strongly dependent on the reduction conditions (it is in fact easier to abstract oxygen from the ceria surface than from the bulk (2, 37)) and on the dimensions of CeO_2 particles. The equilibrium

$$2Ce(IV)_s + 2Ce(IV)_b + O_s + O_b$$

$$\text{LTR} \uparrow\downarrow +H_2(-H_2O)$$

$$2Ce(III)_s + 2Ce(IV)_b + V_{\ddot{o}_s} + O_b$$

$$\text{HTR} \uparrow\downarrow +H_2(-H_2O)$$

$$2Ce(III)_s + 2Ce(III)_b + V_{\ddot{o}_s} + V_{\ddot{o}_b}$$

can be pictured, in which the subscripts s and b stand for surface and bulk, respectively, and $V_{\ddot{o}}$ indicates an oxygen vacancy. The critical parameters affecting the equilibrium are in our case the reduction temperature and the dimension of the CeO_2 crystallites. In the presence of Rh, the first step occurs at relatively low temperatures (below 450 K), while for the second step a stronger reductive environment is needed. Besides, large CeO_2 crystallites must be present to provide bulk Ce(IV) available for reduction. As quantitative TPR and TEM measurements show, with crystallites smaller than 80 Å almost all the Ce(IV) is reduced to Ce(III) after a LTR, while higher temperatures are needed to reduce bulk CeO_2 in bigger particles. As can be seen from Fig. 4 the difference between a LTR and a HTR for $Rh/CeO_2(28.4\%)/SiO_2$ is mainly concentrated in the reduction of bulk CeO_2. Since it is known that the presence of surface Ce(III) and its electronic interaction with noble metals contribute to activate CO moieties (5, 13, 33), the role of the formation of bulk Ce(III) in the observed catalytic properties would be that of providing additional oxygen vacancies to the surface through a migration process. Besides, the presence of oxygen vacancies distributed through all the sample (or more probably a gradient of vacancy concentration from the surface to the bulk) could create the additional driving force for activation of the CO moiety.

The role of oxygen migration in CO oxidation over Rh/CeO_2 has recently been emphasized. Zafris and Gorte (38) have found compelling evidence which indicates the important role of oxygen migration from CeO_2 to Rh in the enhancement of catalytic activity of Rh/CeO_2 catalyst in CO oxidation. Thus, in a strong reduction environment (as during a high temperature reduction) the bulk of the oxide behaves as an oxygen reservoir, supplying oxygen to the surface through a migration process for the reduction process, and under less reductive environment, as during CO_2 methanation, the opposite process is likely to occur: the lattice oxygen is replenished by oxygen from CO_2 dissociation by a diffusion mechanism, thus filling up the vacancies formed during reduction. Since bulk oxygen vacancies are limited, and during CO_2 methanation the reduction conditions are milder (temp. <500 K, low H_2 content, presence of CO_2 and H_2O), it is not possible to regenerate bulk vacancies; as a consequence the annihilation of bulk vacancies under reaction conditions is permanent and the catalytic activity shows a transient behaviour. To regenerate those vacancies and the related catalytic activity another high temperature reduction cycle is needed. By integrating the CH_4 vs time curve reported in Fig. 7 for the $Rh/CeO_2(28.4\%)/SiO_2$ sample after HTR, a quantitative estimate of total CH_4 formed can be made (which is identical to CO_2 reacted). This corresponds to 23.9 μmol $CH_4/g_{cat.}$ formed after 35 min of reaction. By keeping in mind the stoichiometry found for CeO_x after LTR and HTR in the $Rh/CeO_2(28.4\%)/SiO_2$ sample, and by assuming (from Fig. 4) that all the difference is concentrated in the bulk, we have a total of 82.3 μmol of bulk Ce(III)/gCeO$_2$ which are formed after HTR. The oxidation of this amount requires 20.5 μmol of CO_2, a value which is very close to the 23.9 μmol found.

If bulk vacancies cannot be formed, as in the more disperse samples, there is no observable enhancement in the catalytic activity after a HTR. Moreover, the higher CeO_2 dispersion obtained for the less concentrated samples can provide more surface Ce(III), thus accounting for the higher steady-state activity of these catalysts in comparison to undoped Rh/SiO_2 and $Rh/CeO_2(>5.8\%)/SiO_2$. A similar enhancement in CO oxidation was also observed in prereduced $Pt/CeO_2/Al_2O_3$ catalyst in comparison to Pt/Al_2O_3 (39). In this case the presence of vacant sites at the interface between Pt and reduced CeO_2 was proposed to account for the activity enhancement.

It has also been reported that H_2 treatment at high temperature of CeO_2 gives rise to formation of cerium hydride (20) or bronzelike species of the type CeO_2H_x (40), thus increasing the amount of H_2 chemisorbed at high temperatures. The presence of such hydrides had no observable effect on the transient behaviour of Rh/CeO_2 and CeO_2 after a high temperature reduction, as we have previously reported (13). However, a possible role of such species in changing the surface H_2/CO_2 ratio cannot be excluded.

The important relevant implication emerging from these results is that the bulk of the oxide is directly involved in the surface reaction. The role of bulk properties of materials in heterogeneous catalysis has already been investigated by several authors in different reactions. For example, in polyoxoanion chemistry several examples of bulk-type catalysis have been observed, in which, although the main reaction proceeds on the surface, due to rapid diffusion of redox carriers, the whole bulk participates in the reaction (41). Moreover, very interesting

studies investigating the role of defect chemistry and bulk transportation process on surface catalytic chemistry have recently appeared (42). The multivalent character of cerium, which is expected to promote surface and bulk O_2 mobility, is generally recognized as an important feature in several cerium-promoted oxidation reactions (from the CO/NO reaction to propylene ammoxidation) (43). However, we have also seen that under a more reductive environment, such as during CO_2 hydrogenation, a similar mechanism may be operative, although only in transient conditions.

Another relevant implication that can be drawn from these results is the possibility of creating and stabilizing bulk oxygen vacancies under milder reaction conditions. This can be done for example by doping $CeO_2$with other oxides (like ZrO_2 (44)) or by using anion-deficient fluorite solid solutions [CeO_2–Y_2O_3] in which anion vacancies can be present as structural defects on the "as-synthesized" materials (45). In this way, it could be possible to stabilize bulk Ce(III) under reaction conditions, increasing the catalytic activity also in steady-state conditions, and lowering the temperatures for reduction treatments.

CONCLUSIONS

(i) Under TPR conditions Ce(IV) to Ce(III) reduction in pure CeO_2 is not complete; a formal stoichiometry of $CeO_{1.75}$ has been obtained heating in H_2 at temperature up to 1400 K.

(ii) By supporting CeO_2 on amorphous SiO_2, owing to the formation of smaller CeO_2 crystallites and to the H_2 promoted redispersion effect a complete Ce(IV) to Ce(III) reduction is observed at a temperature of 1000 K.

(iii) The presence of Rh accelerates the redispersion of CeO_2 crystallites and enhances CeO_2 surface reduction through the well known spillover effect.

(iv) Samples promoted with CeO_2 (particularly at low CeO_2 loading) show a high activity in CO_2 methanation relative to that of unpromoted Rh/SiO_2. This is probably related to the presence of surface vacancies at the interface between Rh and reduced CeO_2.

(v) High temperature reduction of Rh/CeO_2 and of $Rh/CeO_2/SiO_2$ (with CeO_2 crystallites larger than 80 Å) has a positive effect on catalytic activity in CO_2 methanation. The presence of bulk vacancies, which are formed in large CeO_2 crystallites after reduction at 773 K (but not after a low temperature reduction), is believed to be the driving force leading to CO_2 activation.

ACKNOWLEDGMENTS

We are particularly grateful to Dr. Jan Kaspar (University of Trieste) for reading the manuscript and for giving very helpful suggestions and comments. We also thank Dr. Fabio Miani for carrying out XRD measurements. The authors also thank MURST (40%, 60%) and CNR for financial support. J.LL. acknowledges financial support from CICYT MAT93-0477.

REFERENCES

1. Summers, J. C., and Ausen, A., *J. Catal.* **58,** 131 (1979).
2. Yao, M. D., and Yao, Y. Y. F., *J. Catal.* **86,** 254 (1984).
3. Numan, J. G., Robota, H. J., Cohn, M. J., and Bradley, S. A., *J. Catal.* **133,** 309 (1992).
4. Suddhakar, C., and Vannice, M. A., *Appl. Catal.* **14,** 47 (1985).
5. Suddhakar, C., and Vannice, M. A., *J. Catal.* **95,** 227 (1985).
6. Mendelovici, M., and Steinberg, M., *J. Catal.* **96,** 285 (1985).
7. Cunningham, J., O'Brian, S., Sanz, J., Rojo, J. M., Soria, J. A., and Fierro, J. L. G., *J. Mol. Catal.* **57,** 379 (1990).
8. Harrison, B., Diwell, A. T., and Hallet, C., *Platinum Met. Rev.* **32,** 73 (1988).
9. Le Normand, F., Hilaire, L., Kili, L., Krill, G., and Maire, G., *J. Phys. Chem.* **92,** 2561 (1988).
10. Jin, T., Okuara, T., Mains, G. J., and White, J. M., *J. Phys. Chem.* **91,** 3310 (1987).
11. Trovarelli, A., Mustazza, C., Dolcetti, G., Kaspar, J., and Graziani, M., *Appl. Catal.* **65,** 129 (1990).
12. Trovarelli, A., de Leitenburg, C., and Dolcetti, G., *J. Chem. Soc., Chem. Commun.*, 472 (1991).
13. Trovarelli, A., Dolcetti, G., de Leitenburg, C., Kaspar, J., Finetti, P., and Santoni, A., *J. Chem. Soc., Faraday Trans.* **88,** 1311 (1992).
14. Trovarelli, A., Dolcetti, G., de Leitenburg, C. and Kaspar, J., *Stud. Surf. Sci. Catal.* **75,** 2781 (1993).
15. Mori, T., Masuda, H., Imai, H., Miyamoto, A., Baba, S., and Murakami, Y., *J. Phys. Chem.* **86,** 2753 (1982).
16. Gentry, S. J., Hurst, N. W., and Jones, A., *J. Chem. Soc., Faraday Trans. 1* **77,** 603 (1981).
17. Vis, J. C., van't Blik, H., F. J., Huizinga, T., van Grondelle, J., and Prins, R., *J. Catal.* **95,** 333 (1985).
18. Zotin, F. M. Z., Tournayan, L., Varloud, J., Perrichon, V., and Frety, R., *Appl. Catal. A: Gen.* **98,** 99 (1993).
19. Ricken, M., Nolting, J., and Riess, I., *J. Solid. State Chem.* **54,** 89 (1984).
20. Cunningham, J., Cullinane, D., Sanz, J., Rojo, J. M., Soria, X. A., and Fierro, J. L. G., *J. Chem. Soc., Faraday Trans.* **88,** 3233 (1992).
21. Bernal, S., Calvino, J. J., Cifredo, G. A., Rodriguez Izquierdo, J. M., Perrichon, V., and Laachir, A., *J. Catal.* **137,** 1 (1992).
22. Kepinsky, L., and Wolcyrz, M., *Catal. Lett.* **15,** 329 (1992).
23. Chojnocki, T., Krause, K., and Schmidt, L. D., *J. Catal.* **128,** 161 (1991).
24. Krause, K., Schabes-Retchkiman, P., and Schmidt, L. D., *J. Catal.* **134,** 204 (1992).
25. Bernal, S., Botana, F. J., Calvino, J. J., Cauqui, M. A., Cifredo, G. A., Jobacho, A., Pintado, J. M., and Rodriguez-Izquierdo, J. M., *J. Phys. Chem.* **97,** 4118 (1993).
26. Johnson, M. F. L., and Mooi, J., *J. Catal.* **103,** 502 (1987).
27. Tournayan, L., Marcilio, N. R., and Frety, R., *Appl. Catal.* **78,** 31 (1991).
28. Laachir, A., Perrichon, V., Badri, A., Lamotte, J., Catherine, E., Lavalley, J. C., Fallah, J. E., Hilaire, L., le Normand, F., Quémére, E., Sauvion, G. N., and Touret, O., *J. Chem. Soc., Faraday Trans.* **87,** 1601 (1991).
29. Shyn, J. Z., Weber, W. H., and Gandhi, H. S., *J. Phys. Chem.* **92,** 4964 (1988).
30. Ayers, W. M. (Ed.), "Catalytic Activation of Carbon Dioxide," ACS Symposium Series Vol. 363. American Chemical Society, Washington, DC, 1988; Solymosi, F., *J. Mol. Catal.* **65,** 337 (1991) and references therein.

31. Solymosi, F., and Erdöhelyi, A., *J. Mol. Catal.* **8,** 471 (1980); Solymosi, F., Erdöhelyi, A., and Bansagi, T., *J. Catal.* **68,** 371, (1981).
32. Kienneman, A., Raymond, B., Hindermann, J. P., and Laurin, M., *J. Chem. Soc., Faraday Trans. 1* **83,** 2119 (1987).
33. Rieck, J. S., and Bell, A. T., *J. Catal.* **99,** 278 (1986).
34. Lavalley, J. C., Saussey, J., Lamotte, J., Breault, R., Hindermann, J. P., and Kiennemann, A., *J. Phys. Chem.* **94,** 5941 (1990).
35. Burch, R., and Flambard, A. R., *J. Catal.* **78,** 389 (1982).
36. Tauster, S. J., Fung, S. C., and Garten, R. L., *J. Am. Chem. Soc.* **100,** 170 (1978).
37. Sayle, T. X. T., Parker, S. C., Richard, C., and Catlow, A., *J. Chem. Soc., Chem. Commun.,* 977 (1992).
38. Zafris, G. S., and Gorte, R. J., *J. Catal.* **139,** 561 (1993); Zafris, G. S., and Gorte, R. J., *J. Catal.* **143,** 86 (1993).
39. Serre, C., Garin, F., Belot, G., and Maire, G., *J. Catal.* **141,** 9 (1993).
40. Fierro, J. L. G., Soria, J., Sanz, J., and Rojo, J. M., *J. Solid State Chem.* **66,** 154 (1987).
41. Misono, M., *Stud. Surf. Sci. Catal.* **75,** 69 (1993).
42. Maire, J., *Angew. Chem.* **32,** 313, 528 (1993); Illet, D. J., and Islam, M. S., *J. Chem. Soc., Faraday Trans.* **89,** 3833 (1993).
43. Bradzil, J. F., *in* "Characterization of Catalytic Materials" (I. E. Wachs, Ed.), p 47. Butterworth-Heinemann, Manning, 1992.
44. Ranga Rao, G., Kaspar, J., Di Monte, R., Meriani, S., and Graziani, M., *Catal. Lett.* **24,** 107 (1994); Fornasiero, P., Di Monte, R., Ranga Rao, G., Kašpar, J., Meriani, S., Trovarelli, A., and Graziani, M., *J. Catal.,* **151,** 168(1995).
45. Kilner, J. A., and Steele, B. C. H., *in* "Nonstoichiometric Oxides" (O. T. Sorensen, Ed.), p. 233. Academic Press, New York, 1981.